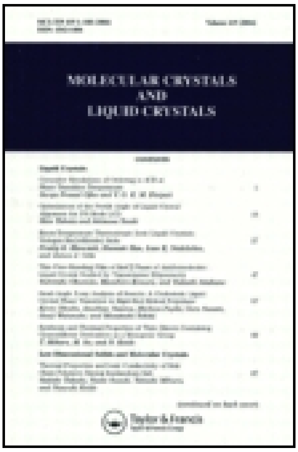

Molecular Crystals and Liquid Crystals Science and Technology. Section A. Molecular Crystals and Liquid Crystals

Publication details, including instructions for authors and subscription information:
http://www.tandfonline.com/loi/gmcl19

Low Energy Excitons in Solid C_{60}

C. Taliani [a] , M. Muccini [a] , R. Zamboni [a] & F. Kajzar [b]

[a] Istituto Spettroscopia Molecolare del C.N.R., via P. Gobetii, 101 - 40129, Bologm, Italy

[b] Commissarrat à l'Energie Atomique, Direction des Technologies Avancées LETI, DEIN/LPEM CEN Saclay, 91191 Gif sur, Yvette Cedex, France

Version of record first published: 04 Oct 2006.

To cite this article: C. Taliani , M. Muccini , R. Zamboni & F. Kajzar (1994): Low Energy Excitons in Solid C_{60} , Molecular Crystals and Liquid Crystals Science and Technology. Section A. Molecular Crystals and Liquid Crystals, 256:1, 187-198

To link to this article: http://dx.doi.org/10.1080/10587259408039247

Mol. Cryst. Liq. Cryst. 1994, Vol. 256, pp. 187–198
Reprints available directly from the publisher
Photocopying permitted by license only

LOW ENERGY EXCITONS IN SOLID C_{60}

C. TALIANI†, M. MUCCINI†, R. ZAMBONI† AND F. KAJZAR*

*†Istituto di Spettroscopia Molecolare del C.N.R., via P. Gobetti, 101 - 40129 Bologna, Italy. *Commissariat à l'Energie Atomique, Direction des Technologies Avancées LETI, DEIN/LPEM, CEN Saclay, 91191 Gif sur Yvette Cedex, France.*

Abstract. Both the exceptional high symmetry of the C_{60} molecule and the molecular nature of the solid determine the conditions for a dipole forbidden lowest excited electronic manifold which extends from 1.8eV to about 3eV. The one-photon activity in this spectral range is due to the Herzberg-Teller vibronic coupling between these forbidden states and higher T_{1u} excitations. The location of the lowest excited singlet state is performed by two non-linear spectroscopic techniques. First we report on the third harmonic generation spectrum of C_{60} thin film. Fitting of the relatively large number of experimental points with a three-level model suggests the presence of a low lying forbidden state at 1.87 eV. Preliminary data of two-photon excitation spectroscopy of C_{60} single crystal confirm this finding and allows to locate the level at 1.846 eV. This is in complete agreement with the assignment to a T_{1g} excited state based on the photoluminescence experiments presented by Guss et al. in this issue.

1. INTRODUCTION

The molecular nature of C_{60} is well established by the many experimental results of the last few years. One of the most convincing evidence is given by the electronic absorption spectrum. The spectrum of a thin film was reported for the first time by Krätschmer et al. /1/. The absorption spectrum consists of a very weak and broad system extending from 1.9 to 2.7 eV (650-450 nm) and of a series of sharp bands at 3.65 eV (339 nm), 4.70 eV (264 nm) and 5.74 eV (216 nm). The solution spectrum /2/ is very similar to the solid spectrum /1,3,4/ and has been analyzed in terms of Herzberg-Teller vibronic coupling /5/.

The similarity between the spectra of isolated molecules and the solid implicates that the intermolecular interactions are weak, due to Van der Waals forces, and therefore the solid is a typical molecular crystal. Neutral electronic excitations of the molecule give rise therefore to tight-binding Frenkel excitons in the solid /6/. The forbidden nature of the low lying excitations in C_{60} makes it impossible to locate directly the electronic origin. In this paper we report on the identification of the low energy excitations in solid

C_{60} by means of non-linear spectroscopies. In paragraph 1.1 we give a short summary of the sequence of electronic excited states in the free molecule based on quantum-chemical calculations. Subsequently in paragraph 1.2 we discuss on the Herzberg-Teller coupling effect. In paragraph 1.3 and 1.4 we treat the two experimental approaches by means of non-linear spectroscopies, namely third harmonic generation (THG) spectroscopy and two-photon excitation (TPE) spectroscopy.

1.1 Excited states in the isolated C_{60} molecule

The electronic energetics of fullerene C_{60} is determined by the 60 electrons on p orbitals, one on each carbon atom, while the cage is formed by the overlap of sp^2 hybridized orbitals. Each p orbital makes a small angle with adjacent orbitals (23.2 deg). The overlap between orbitals allows therefore the formation of an extended π electronic system.

Using one-electron description of the electronic structure, according to the Hückel molecular orbital approach, one gets a close shell system with a considerable gap between HOMO (highest occupied molecular orbital) and LUMO (lowest unoccupied molecular orbital) orbitals. Furthermore the high symmetry of the molecule, gives rise to a large degeneracy of the molecular orbitals.

The schematic representation of the molecular orbitals obtained by this very simple approach is shown in Fig. 1.

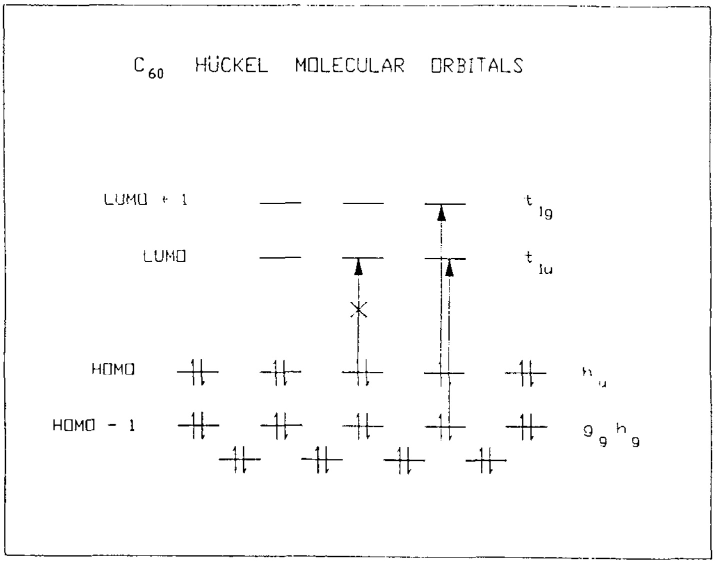

Fig 1. Hückel molecular orbitals of C_{60}. Only the orbitals relevant for the low energy excitations are shown.

Electronic promotion from HOMO (h_u) to LUMO (t_{1u}) is forbidden for electric dipole operator and therefore it is forbidden for linear optical absorption, while promotions from HOMO-1 (g_g, h_g) to LUMO and HOMO to LUMO+1 (t_{1g}) are allowed. A more rigorous treatment of the electronic structure should include Coulomb interactions. In fact, in π conjugated molecules, it has been recognized long ago /7/ that inclusion of e-e correlation is essential to reproduce the low energy excitations. Semiempirical Hartree-Fock quantum chemical calculations parametrized for treatment of π electrons /5/ gives a sequence of states which is reported in Table 1. This treatment has been implemented for the description of π electrons allowing to get generally a qualitatively good description of the sequence of the excited states transitions. In the multi-electron approach, the electronic states are classified according to the molecular point group which, in the case of the hycosahedral C_{60} molecule, is I_h

Total Symmetry of the wf	Energy (eV)	Intensity (f)
$1T_{2g}$	2.29	
$1T_{1g}$	2.33	
$1G_g$	2.34	
$1H_g$	2.65	
$1T_{2u}$	2.76	
$1H_u$	3.01	
$1G_u$	3.11	
$1T_{1u}$	3.36	0.12
$2G_u$	3.38	
$2H_u$	3.70	
$2T_{1u}$	4.00	0.63
$3T_{1u}$	4.26	2.46
$4T_{1u}$	4.59	0.75
$5T_{1u}$	4.97	4.83

Table 1. Energies of the lowest electronic states of C_{60} calculated by CNDO/S (up to 5 eV) configuration interaction (CI) taking 1295 configurations. The last column indicates the oscillator strength (f) [from Ref. 5].

1.2 Forbidden states and Herzberg-Teller coupling

Since the ground state of the free molecule is totally symmetric (A_g character), the low energy excitations are dipole forbidden since the lowest states transform like irreducible representations of gerade symmetry (T_{2g}, T_{1g}, G_g, H_g). The only dipole allowed transition is from the ground state to states of T_{1u} symmetry.

There are several $T_{1u} \leftarrow A_g$ transitions which have increasing oscillator strenght by going towards higher energies (see last column of Table 1). The broad region at about 2.00 eV was identified by many investigators /2,3,4,5,8/ to be the region of forbidden transitions.

It is well known that selection rules of transitions from the ground state to excited states may be derived from the solution of the direct product of irreducible representation of the ground and excited state wave functions (*wfs)* and the electric dipole operator. The transition matrix element $<\Phi_g | \mathbf{er} | \Phi_e>$ is nonzero [where Φ_g and Φ_e are the ground and excited states respectively and **er** is the electric dipole operator] if the direct product contains the totally symmetric representation. Therefore:

$$\Gamma_g \otimes \Gamma_m \otimes \Gamma_e = A_g \qquad (1)$$

where Γ_g is the representation of the ground state *wf* (A_g) and Γ_e is the representation of the excited state *wf*.

In the case of the I_h point group, the electric dipole operator Γ_m, transforms like the T_{1u} representation and the direct product does not contain A_g making the transition matrix element equal to zero. In fact:

$$A_g \otimes T_{1u} \otimes T_{1g} \neq A_g \qquad \text{i.e.} \qquad <A_g | \mathbf{er} | T_{1g}> = 0 \qquad (2)$$

The mechanism that is active in making these, formally forbidden transitions, observable in absorption, is the Herberg-Teller (H-T) coupling /9/. Allowing the transition moment to depend on the nuclear normal coordinates Q, the transition from the ground state A_g to a vibronic level of the excited T_{1g} state, may acquire some intensity by borrowing it from higher energy allowed transitions ($n^1T_{1g} \leftarrow 1^1A_g$).

The H-T vibronic mechanism implies that transitions between two states may occour with a finite probability at nuclear coordinates away from the equilibrium geometry for particular normal coordinates of appropriate symmetry.

The selection rule that governs the H-T vibronic coupling is the following:

$$\Gamma_g \otimes \Gamma_m \otimes \Gamma_e \otimes \Gamma_v = A_g \qquad (3)$$

where $\Phi_e \varphi_v$ is the total vibronic *wf* of the excited state (Φ_e=electronic *wf*; φ_v= vibrational *wf*) involved in the transition and Γ_v is the representation of the vibrational *wf*. In the case in which $\Gamma_g = A_g$ and $\Gamma_e = T_{1g}$, the vibrations which are active in the H-T coupling belong to the symmetry representations a_u, t_{1u} and h_u. In the case for instance of vibration of t_{1u} symmetry the total direct product is the following:

$$A_g \otimes T_{1u} \otimes T_{1g} \otimes t_{1u} = A_g \tag{4}$$

and therefore the transition matrix element is non zero:

$$\langle A_g | er | T_{1g} t_{1u} \rangle \neq 0 \tag{5}$$

In conclusion, while the purely electronic transition $1^1T_{1g} \leftarrow 1^1A_g$ is still forbidden, the transition to the vibronic level $T_{1g}t_{1u}$, is allowed. This transition is called a "false origin". By expressing the electronic Hamiltonian H as:

$$H = H^\circ + \sum_K \left(\frac{\delta H}{\delta Q_K} \right) Q_K + \ldots \tag{6}$$

For small dispacements, the second term of the Hamiltonian acts as a perturbation and Q_k is a normal coordinate. The adiabatic *wfs* of the excited state$\Phi_e(q,Q)$, where q and Q are the electronic and nuclear coordinates respectively, are expanded over diabatic zero-order *wfs* :

$$\Phi_j = \sum_i c_{ij}(Q)\, \Phi_i^\circ \tag{7}$$

The intensities of H-T active transitions to vibronic levels may therefore be calculated by evaluating the expansion coefficients c_{ij}. These have been calculated by Negri et al. /5/ with a CNDO/S Hamiltonian. It turns out that the most active H-T vibrations in the case of $1^1T_{1g} \leftarrow 1^1A_g$ transitions are the following:

mode	calc.	exp	$f \times 10^4$
t_{1u}	1437	1429	75
	1212	1183	6
h_u	1646		19
	1269		6
	724		3
	403		5

Table 2. CNDO/S calculated oscillator strengths of the H-T false origins for the $1T_{1g}$ singlet state in C_{60}. From Ref. /5/.

Two major false origins are expected to occour in absorption to the $1T_{1g}$ state. The photoluminescence (PL) spectrum of C_{60} single crystal has been analyzed in this framework /10/ and it has been shown indeed that the relative intensities of the PL bands may be interpreted in terms of t_{1u} (1437 cm^{-1}) and h_u (1646 cm^{-1}) false origins of a $1^1T_{1g} \leftarrow 1^1A_g$ transition. This experiment sets the phonon-less electronic origin at 15089 cm^{-1} (i.e. 1.871 eV) which is not observed in linear spectroscopy.

A direct determination of the origin can be made by means of non-linear spectroscopic techniques.

1.3 Third harmonic generation spectroscopy (THG)

By illuminating a thin film of C_{60} with a tunable laser beam and investigating the dependence of the third harmonic intensity upon the tilting angle of the film one may derive the third order electric susceptibility $\chi^{(3)}(-3\omega;\omega,\omega,\omega)$ which, from time dependent perturbation approach /11,12/, is given by the following expression:

$$\chi^{(3)}(-3\omega;\omega,\omega,\omega)\ \alpha\ e^4 \sum_{n\neq g}\sum_{m\neq g}\sum_{l\neq g} f_{gn}f_{nm}f_{ml}f_{lg}\ x$$

$$\left[\frac{1}{(E_{ng}-3\omega)(E_{mg}-2\omega)(E_{lg}-\omega)} - \frac{1}{(E_{ng}+\omega)(E_{mg}-2\omega)(E_{lg}-\omega)} + \frac{1}{(E_{ng}+3\omega)(E_{mg}+2\omega)(E_{lg}\pm\omega)} - \frac{1}{(E_{ng}+\omega)(E_{mg}+2\omega)(E_{lg}-\omega)}\right] \tag{8}$$

where f_{ij} are the transition matrix elements between states i and j, and E_{ij} are the energies of these transitions and ω is the photon energy of the incoming beam.

It is evident that $\chi^{(3)}$ depends critically on the energy denominators. When the energy of the incoming photon is three times lower than the energy of the allowed transition from the ground state to an excited state, one expects a peak in the THG spectrum. This resonance is then a three-photon resonance. On the other hand if the energy of the incoming beam is two times lower than the energy of a two-photon allowed transition there will be a resonance in the $\chi^{(3)}(-3\omega;\omega,\omega,\omega)$ spectrum. This is therefore a so called two-photon resonance effect. These resonance effects are schematically shown in Fig. 2. THG could therefore be used as a tool to search for two-photon states. Experimental details are reported in previous papers /13,14/. In essence a tunable infrared laser beam illuminates a thin film of C_{60} on a silica substrate and the outgoing third harmonic intensity is measured as a function of the incident angle. Fitting of the angle dependence of the THG of the substrate and of the film plus substrate gives the cubic susceptibility $\chi^{(3)}(-3\omega;\omega,\omega,\omega)$.

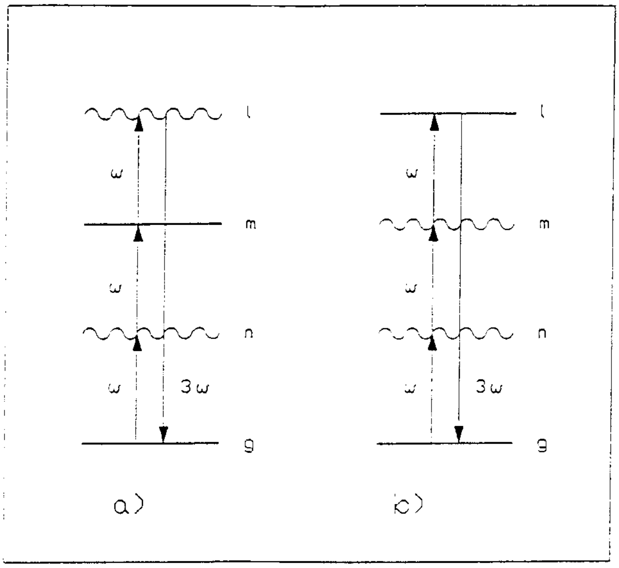

Fig. 2. Schematic energy level diagram for a) third harmonic generation (THG) assisted by a three-photon resonance; b) THG assisted by a two-photon resonance.

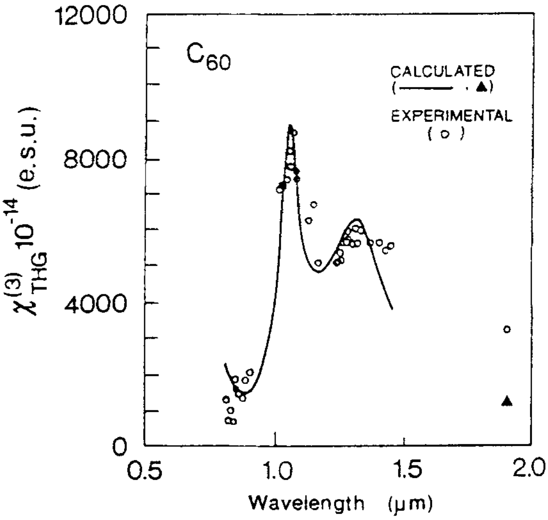

Fig. 3. Third harmonic generation spectrum of C_{60} thin film (dotted line). The full line represents a fitting by using a three-level model.

The measured cubic susceptibility $\chi^{(3)}$ $(-3\omega;\omega,\omega,\omega)$ is plotted in Fig. 3 as function of fundamental laser wavelength. A total of 43 experimental points have been measured in the range of 0.8-1.907 μm (1.54 - 0.65 eV) fundamental wavelength /15/. The relative precision in the $\chi^{(3)}(-3\omega;\omega,\omega,\omega)$ determination is 2-3% within the spectral range of emission of the individual dyes.

From Fig. 3 we observe that, besides the broad resonance at about 1.3 μm (0.95 eV), a second sharper resonance in the $\chi^{(3)}$ $(-3\omega;\omega,\omega,\omega)$ spectrum exists at about 1.06 μm (1.17 eV). The first resonance was already reported by us /13,14/ and by Meth et al. /16/.

The resonance at 1.064 μm (1.165 eV) is clearly a three-photon resonance, the triple of the fundamental photon energy being equal to the T_{1u} one-photon allowed transition at 3.5 eV. The second broad resonance at around 1.3 μm falls in the range of a significantly weaker one-photon absorption with a characteristic appearance of forbidden transitions made partially allowed by H-T coupling. We therefore assigned the maximum of the THG spectrum at 441 nm harmonic wavelength, or 1.323 μm fundamental wavelength (see Fig. 2) to a two-photon resonance with the electronic origin of the T_{1g} forbidden state located in the solid at 1.87 eV /15/. The zero-phonon electronic origin, which is not observed by direct linear absorption, should be located at slightly lower energy than the false origins which are responsible of the weak absorption. The energy difference being that of the vibration involved in the vibronic coupling (see paragraph 1.2). From our measurements we locate the lowest T_{1g} level at 1.87 eV which is in fair agreement within the experimental accuracy of our experiment. Possible three-photon resonant contributions from vibronic levels of total T_{1u} character (i.e. false origins or progression built on it) may also contribute to the envelope of the THG feature.

In order to take into account the frequency variation of the cubic susceptibility we consider a simple three-level model with two gerade and one ungerade states. According to Orr and Ward /11/ the cubic susceptibility, in the framework of this model, is given by:

$$\chi^{(3)}(-3\omega;\omega,\omega,\omega) = 3\pi^2 \, Nf|\mu_{01}|^2/4h^3 \, [\, |\mu_{12}|^2 \, F(\omega_1, \omega_2, \Gamma_1, \Gamma_2) - \\ - |\mu_{01}|^2 \, G(\omega_1, \omega_2, \Gamma_1, \Gamma_2)] \tag{9}$$

where N is the density of molecules, *f* is the local field factor, ω_i are transition energies between fundamental and excited states of opposite (i=1) and the same (i=2) parity, Γ_i are the corresponding damping terms and μ_{01}, μ_{12} are dipolar transition moments between fundamental and one-photon and two-photon allowed levels, respectively. The functions $F(\omega_1, \omega_2, \Gamma_1, \Gamma_2)$ and $G(\omega_1, \omega_2, \Gamma_1, \Gamma_2)$ describe the dispersion of cubic susceptibility and their exact form can be found in Ref. /15a/. Equation (9) has been least square fitted to experimental data. The best fit has been obtained with reasonable values of free parameters:

$\omega_1 = 350$ nm , $\omega_2 = 660$ nm , $\Gamma_1 = 814$ cm^{-1}, $\Gamma_2 = 1178$ cm^{-1}, $\mu_{01} = 25.3$ D and $\mu_{12} = 26.3$ D

The calculated dispersion is plotted as a solid line in Fig. 3. An overall good agreement between measured and calculated values is observed. Quantum chemical calculation /5/ indicates a congestion of forbidden electronic levels made partially allowed by vibronic coupling with higher T_{1u} levels. All these levels fall within the investigated spectral range and may contribute to the resultant susceptibility $\chi^{(3)}$ $(-3\omega;\omega,\omega,\omega)$. Theoretically it is possible to include all these transitions into the computation, but the use of a large number of free parameters may improve the fitting but not the physical meaning of it.

A simple three-level model allows therefore to assign the second resonance to a two-photon resonance with the low lying gerade T_{1g} state at 1.87 eV. The simplicity of the three-level model considered here indicates undoubtely a low lying gerade state. Nevertheless its precise location requires a direct probe of the state by two-photon absorption (see next paragraph).

1.4 Two-Photon Excitation Spectroscopy (TPE)

In this paragraph we report on preliminary investigations on the direct location of the lowest singlet exciton band by two-photon excitation (TPE) spectroscopy on the C_{60} single crystal at liquid helium temperature.

Photogeneration of singlet exciton via a two-photon absorption process will quickly lead (10^{-13}s) to trapping of the excitation into the manifold of X-traps and subsequent radiative photoemission, which have been previously identified in the single crystal /10/. We assume that the quantum yield of this radiative relaxation process is independent on the energy of the exciting photon. Under these conditions we may derive the relative two-photon absorption intensity from the intensity of the photoluminescence detected for each pulse.

C_{60} possesses at low temperature a simple cubic (sc) phase with four inequivalent molecules per unit cel located at 0,0,0; 0,1/2,1/2; 1/2,0,1/2; 1/2,1/2,0 positions. The crystal *wfs*, that are generated as linear combination of molecular *wfs* of the non equivalent molecules in the unit cell, belong to the symmetry of the factor group which is isomorphous with the space group /6b,6c/.

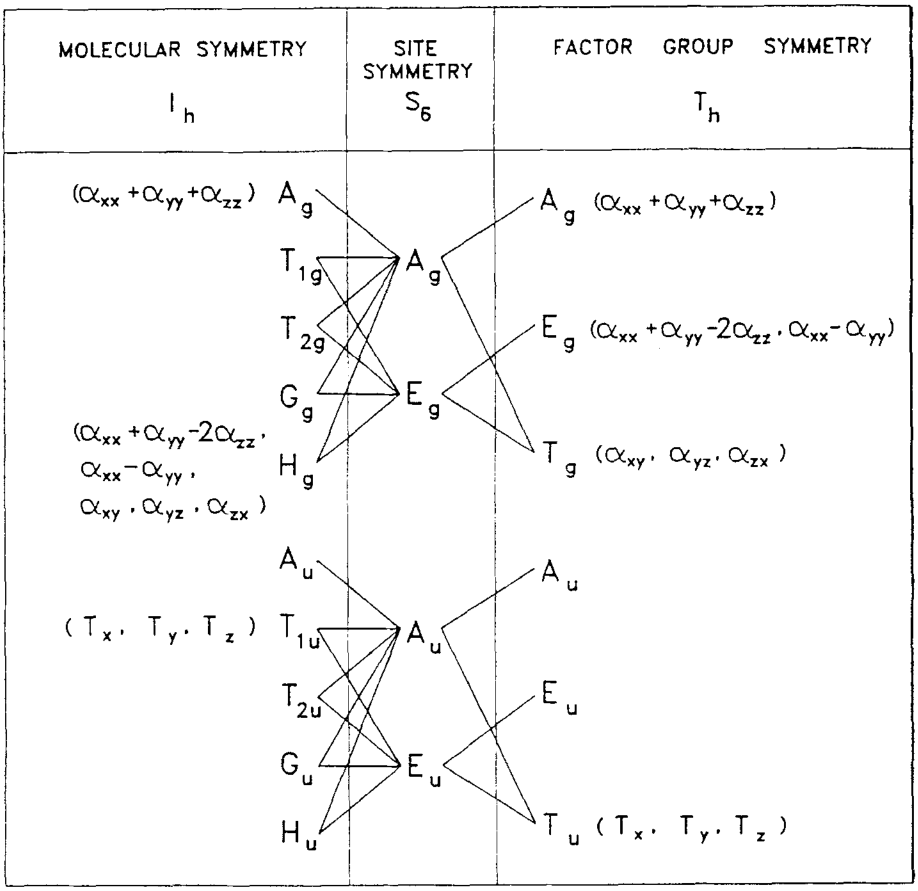

Fig. 4. Correlation diagram of the I_h Point group of the isolated C_{60} molecule with the Factor group for solid C_{60} via the S_6 Site symmetry.

The correlation among the symmetry of the free molecular *wfs* and the symmetry of the crystal *wfs* is shown in Fig.4. Since the site symmetry is S_6 each molecular irreducible representation on the left side of Fig. 4 correlates via the Site group symmetry (center) to the irreducible representation of the crystal in a way which preserves the parity character. The correlation is indicated by the lines. The T_{1g} (molecular) for instance, correlates with A_g, E_g and T_g (Factor). Since in the T_h point group these representations transform like polarizability tensor components then the T_{1g} level, which is two-photon forbidden in the free molecule, become partially allowed in the crystal due to this correlation effect which is also known as crystal field effect.

Taking advantage of this effect it is therefore possible to locate the lowest forbidden singlet by two-photon excitation.

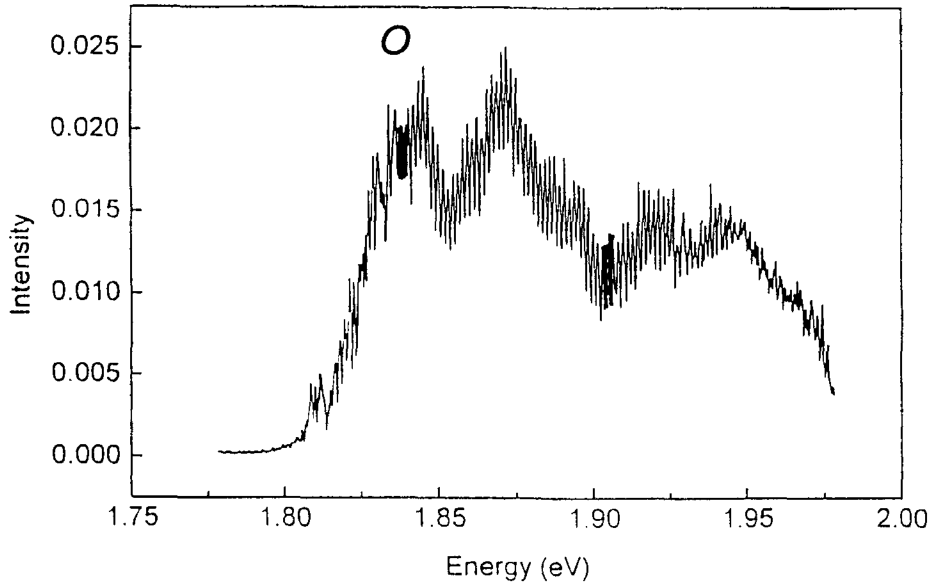

Fig. 5. Two-photon excitation spectrum of C_{60} single crystal at 4.2K. The photon energies given in abscissa are at twice the energy of the laser photon and indicate therefore the energy of the electronic levels.

The low-temperature TPE spectrum of C_{60} single crystal is reported in Fig. 5. The spectrum does not show any feature in the range of 1.7-1.8 eV, which is the spectral range of the main peaks observed in the photoluminescence spectrum of the single crystal performed by W Guss et al. /10/. The first band indicated by O is at 1.846 eV (14889 cm^{-1}). O marks the origin of the TPE spectrum and is assigned to a pure electronic transition (zero-phonon transition of the k=0 Frenkel singlet exciton). It indicates the bottom of the lowest singlet Frenkel exciton band. This confirms the indirect evidence from THG spectroscopy (vide supra). By comparing these results with those obtained by photoluminescence /10/ it is possible to unambiguosly assign the lowest energy Frenkel exciton to the T_{1g} state.

Acknowledgment

The skillful technical assistance of G. Tasini, P. Mei and A. Martiniello is acknowledged. This work was partly supported by the European Commission ESPRIT Basic Research Action 8013 - LEDFOS.

References

1. W. Krätschmer, L.D. Lamb, K. Fostiropoulos and D. R. Huffman, Nature 347, 354 (1990).
2. S. Leach, M. Vervloet, A. Desprès, E. Breheret, J.P. Hare, T.J. Dennis, H.W. Kroto, R. Taylor and D.R.M. Walton, Chem. Phys. 160, 451 (1992).
3. A. Skumanich, Chem. Phys. Lett. 182, 486 (1991).
4. C. Reber, L. Yee, J. MacKiernan, J.I. Zink, R.S. Williams, W. M. Tong, D. A. A. Ohlberg, R.L. Whetten and F. Diederich, J. Phys. Chem. 95, 2127 (1991).
5. F. Negri, G. Orlandi and F. Zerbetto, J. Chem. Phys. 97, 6496 (1992).
6. a) J. Frenkel, Phys. Rev. 37, 17, 1276 (1931); b) A.S. Davydov, *Theory of molecular excitons* (Plenum, New York, 1971); c) D.P. Craig and S.H. Walmsley, *Excitons in molecular crystals* (W.A. Benjamin, Inc. New York, 1968).
7. P.O. Löwdin, Phys. Rev. 97, 1474 (1955).
8. K. Yaban and G.F. Bertsch, Chem. Phys. Lett. 197, 32 (1992).
9. G. Herzberg and E. Teller, Z. Phys. Chem. B 21, 410 (1933).
10. W. Guss, J. Feldmann, E.O. Goebel, C. Taliani, H. Mohn, P. Haeusslerand and H.-U.ter Meer, Phys. Rev. Lett. (in press), (1994).
11. B. J. Orr and J. F. Ward, Mol. Phys. 20, 513 (1971).
12. P.N. Butcher and D. Cotter, *The Elements of Nonlinear Optics*, in Cambridge studies in Modern Optics 9, Cambridge University, Cambridge (1990).
13. F. Kajzar, C. Taliani, R. Zamboni, S, Rossini and R. Danieli, in: Fullerenes: Status and Perspectives, eds. C. Taliani, G. Ruani and R. Zamboni (World Scientific, Singapore, 1992) p. 75.
14. F. Kajzar, C. Taliani, R. Zamboni, S, Rossini and R. Danieli, Synth. Metals 54, 21 (1993).
15. a) F. Kajzar, C. Taliani, R. Zamboni, S, Rossini and R. Danieli, SPIE Proc., 2025 (1993); b) F. Kajzar, C. Taliani, R. Danieli. S. Rossini and R. Zamboni, Chem. Phys. Lett 217, 418 (1994).
16. J. S. Meth, H. Vanherzeele and Y. Wang, Chem. Phys. Lett. 197, 26 (1992).